Effects of multi-scale velocity heterogeneities on wave-equation migration

Yong Ma and Paul Sava, Center for Wave Phenomena, Colorado School of Mines*

SUMMARY

Velocity models used for wavefield-based seismic imaging represent approximations of the velocity characterizing the area under investigation. The real subsurface velocity can at best be approximated by the combination of a known background velocity and unknown multi-scale heterogeneities. Here, we model the multi-scale heterogeneity assuming a fractal behavior and compare this type of heterogeneity with conventional correlated Gaussian random distributions. Data simulated for the various heterogeneity distributions are characterized by spectra with different shapes when analyzed in the log-log domain. For example, Gaussian distributions are characterized by exponential functions and fractal distributions are characterized by linear functions with fractional slopes. These properties hold for both data and migrated images after deconvolution of the source wavelet. Exploiting the distinctions between the various kinds of heterogeneities, we can use least-squares fitting to ascertain characteristics and parameters of heterogeneity from the seismic data and migrated images.

INTRODUCTION

Wave-equation migration consists of two steps (Claerbout, 1985). The first consists of wavefield reconstruction at every location in the subsurface from data recorded at the surface using a numeric solution to a wave equation. The second consists of extracting reflectivity information from the reconstructed wavefields using an imaging condition. The accuracy of wavefield reconstruction, which directly determines the quality of migrated images, depends on the accuracy of both the velocity model and the wave-equation used for wavefield reconstruction.

Conventionally, we decompose the Earth's velocity into two models corresponding to the the large-scale (low-frequency) and to the small-scale (high-frequency) components. We refer to the large-scale component as the velocity model and to the small-scale component as the reflectivity model. The large-scale component of the model is used for wavefield reconstruction, and the small-scale component of the model is the object of the imaging condition. However, real geologic environments do not follow this clear separation of scales. Evidence from well logs and rock outcrops indicates that a better description of the subsurface requires heterogeneity at all scales of variation (Richter-Bernburg, 1987). We refer to this type of models as *multi-scale*. The multi-scale variability is ignored in imaging which usually assumes that the mid-range of variability does not exist. As a consequence, imaging with smooth models leads to inaccurate wavefield reconstruction and to corresponding distortions of migrated images.

Velocity heterogeneity is conventionally treated as random perturbations superposed on a large-scale background distribution (Hoshiba, 2000). An alternative description of mid-scale heterogeneities is based on the fractal character of natural objects, which is documented by many geological and geophysical phenomena, e.g., rock fragments, faults, earthquakes, and well logs (Mandelbrot, 1982; Turcotte, 1997; Dolan et al., 1998). Fractals posses the property of scale invariance which means that they are built using self-similarity relations.

In this paper, we analyze various types of heterogeneity and their impact on seismic data and migrated images. By analyzing spectra in the log-log space, we can extract heterogeneity information characterizing models from data and images.

MODEL HETEROGENEITY

Stratigraphy is conventionally represented in seismic imaging by blocky models, as shown in Figure 1(a). This model marks the main reflectors in the subsurface which are the main target of seismic imaging. Additionally, random fluctuations at various scales (Hoshiba, 2000) can be added to this velocity model, as shown in Figures 1(b)-1(c).

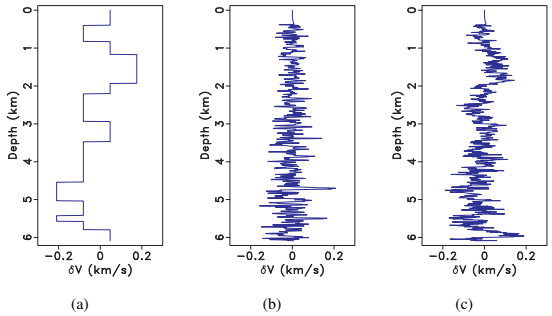

Figure 1: (a) Blocky distributions. (b) Correlated Gaussian random perturbations. (c) Fractal random perturbations.

Gaussian heterogeneity

Mid-scale velocity heterogeneities can be approximated by random distributions. Correlated Gaussian random distributions can be constructed by convolution of uncorrelated random noise $n(x)$ with a Gaussian smoothing function $g(x)$

$$r_g(x) = n(x) * g(x) \ . \tag{1}$$

The Gaussian function $g(x)$ is obtained by inverse Fourier transform of

$$G(k) = e^{-\sigma^2 k^2/4} \ , \tag{2}$$

where σ governs the correlation distance and k represents the wavenumber associated with variable x. By definition, we can relate the wavenumber k with the wavelength by $\lambda = \frac{2\pi}{k}$. Then, we can write

$$G(\lambda) = e^{-\sigma^2 \pi^2/\lambda^2} \ , \tag{3}$$

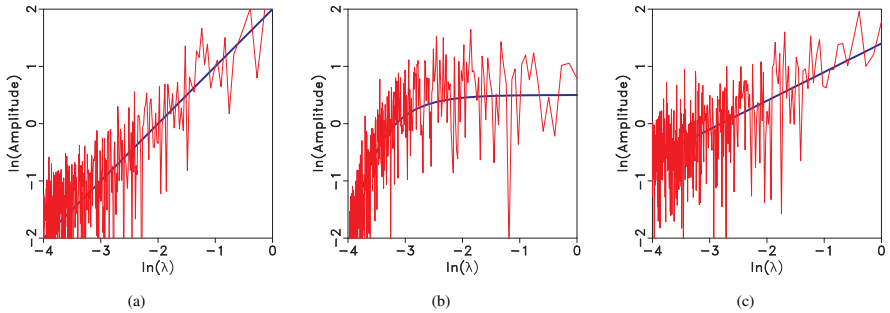

Figure 2: Log-log spectra corresponding to the velocity profiles in Figures 1(a)-1(c), respectively. The thick lines are least-squares fits of the spectra according to linear or exponential laws.

therefore, by taking the natural logarithm, we obtain

$$\ln G = -\pi^2 \sigma^2 e^{-2\ln\lambda} + const\ . \tag{4}$$

The interpretation of equation 4 is that the $\ln G - \ln\lambda$ dependence is exponential. Furthermore, if we observe random noise with this general dependence, then we can conclude that the input signal has Gaussian character. Figure 1(b) shows an example of correlated Gaussian random noise with 10 m correlation in depth.

Fractal heterogeneity

By definition, fractals are quantities characterized by self-similarity (Mandelbrot, 1982). Fractals are often initiated with a large scale generator which is then repeated iteratively at finer scales. For example, for a generator function $l(x)$, a self-similar fractal function has the property

$$l(rx) = l(x)\, r^{Ha}\ , \tag{5}$$

where r is a scaling factor, and Ha is known as the Hausdorff measure which determines the fractal dimension $D = 2 - Ha$ (Turcotte, 1997).

We can construct stochastic self-similar functions by convolution of uncorrelated random noise $n(x)$ with a fractal series $f(x)$

$$r_f(x) = n(x) * f(x)\ . \tag{6}$$

The fractal series $f(x)$ is obtained by inverse Fourier transform of a function with power-law dependence:

$$F(k) = k^{-\beta}\ , \tag{7}$$

where β is related to the fractal dimension D as $\beta = 2.5 - D$ (Turcotte, 1997). Replacing the wavenumber k with the wavelength λ, we can write

$$F(\lambda) = \left(\frac{\lambda}{2\pi}\right)^{\beta}\ , \tag{8}$$

therefore, by taking the natural logarithm, we obtain

$$\ln F = \beta \ln\lambda + const\ . \tag{9}$$

The interpretation of equation 9 is that the $\ln F - \ln\lambda$ dependence is linear. Furthermore, if we observe random noise with this general dependence, then we can conclude that the noise has fractal character. Figure 1(c) shows an example of fractal random noise with power law of order 0.5.

Figures 2(a)-2(c) compares log-log spectra of the blocky velocity with correlated Gaussian random and fractal heterogeneities. Figure 2(a) is the log-log spectrum of the blocky profiles in Figure 1(a). In this spectrum, the thick line represents linear least-squares fit with the regression function $y = \alpha_1 x + \alpha_2$, and in this case the slope of the fit is equal to 1. In contrast, the spatially correlated Gaussian random distribution shown in Figure 2(b) and corresponding to Figure 1(b) matches an exponential trend, as suggested by equation 4 and indicated in the figure by the thick line corresponding to the regression function $y = \alpha_3 e^{-2x} + \alpha_4$. Similarly, the fractal random distribution shown in Figure 2(c) and corresponding to Figure 1(c) matches a linear trend, as suggested by equation 9 and indicated in the figure by the thick line (Stefani and De, 2001). However, the linear slope is different from 1 which distinguishes the fractal profile from the blocky one shown in Figure 2(a). In this case, the linear fit applied to the log-log spectra is characterized by a slope of 0.5.

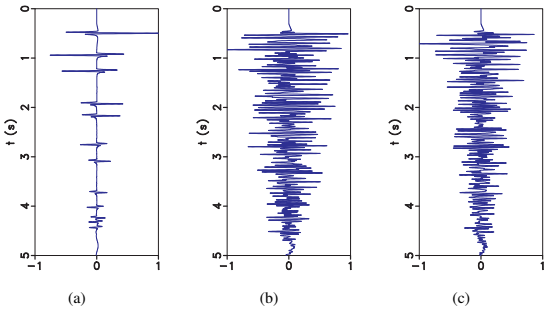

Figure 3: Synthetic seismic data obtained by finite-differences modeling in 1-D models characterized by Figures 1(a)-1(c), respectively.

DATA HETEROGENEITY

Figures 3(a)-3(c) show the data obtained by finite-difference modeling using the velocity models shown in Figures 1(a)-1(c), respectively. We use a central frequency $f = 20$ Hz.

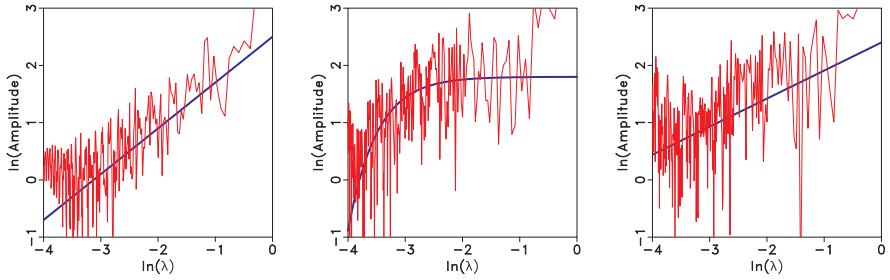

Figure 4: Log-log spectra corresponding to the data in Figures 3(a)-3(c), after deconvolution of the modeling wavelet. The thick lines are least-square fits of the spectra according to linear or exponential laws.

By studying the simulation, we attempt to understand whether the character of the random fluctuation is influenced by wave propagation and whether we can recover information about the random character of the model through direct observations of recorded data.

Assuming that the wavelet is known, at least approximately, we can deconvolve the wavelet from the recorded data and analyze the remaining spectrum to extract information about the model fluctuations. Figures 4(a)-4(c) depict the log-log spectra of reflectivity extracted from data shown in Figures 3(a)-3(c). For example, the spectrum of the blocky model corresponds to a slope close to 1. The spectrum of the data for the model with Gaussian variability shows an exponential trend fitted by parameters $\alpha_3 = -\pi^2\sigma^2 = -0.001$ which implies that $\sigma = 0.01$, indicating a correlation length of about 10 m. The spectrum of the data for the model with fractal variability shows a linear trend fit by parameter $\alpha_1 = 0.49$ which are close to the power order of 0.50, which characterizes the velocity model. These trends are consistent with the trends obtained by analyzing the spectra of the velocity model themselves, which indicates that properties of the random component of the model are preserved in data and can be extracted, assuming that we know the corresponding wavelet with sufficient accuracy.

IMAGE HETEROGENEITY

The analysis performed in the preceding section addresses the question whether we can access information about the model heterogeneity through the analysis of recorded data. In this section we address an alternative question, i.e. whether we can access the same information through analysis of migrated images. For this analysis, we use a portion from a well-log acquired in the field. In this case, we do not know a-priori the nature of the randomness.

Figure 5(a) shows the P-wave velocity constructed from well measurements superimposed on a velocity model obtained as horizontal extension of the well-log. Figure 6(a) shows the log-log spectrum of the well-log. The thick straight line represents the linear least-squares fit applied to the spectrum. The slope is equal to 1 which is consistent with the fact that the well log is dominated by a smooth non-constant background component, or put another way, the spectrum is dominated by a slope inversely proportional with the wavenumber k (Shtatland, 1991). In order to emphasize the heterogeneities present in the model, we first remove the k^{-1} spectrum. In the k domain, according to the nonlinear least-squares fitting $y = ak^{-1}$, we estimate the intensity of the k^{-1} component which corresponds to the background velocity. Because of the linear assumption of velocity model composition, we can apply a linear operation in the k domain, i.e. we subtract the nonlinear least-squares fit from the entire spectrum. After removing the k^{-1} component, we analyze separately the remaining spectrum shown in Figure 6(b). The slope of the linear least-squares fit is equal to 0.53 which, as expected, indicates that the model randomness has a fractal character.

Figure 5(b) shows a simulated shot-record data with a source located at $x = 2.0$ km, $z = 0$ km. The zero-offset trace is superimposed on the data. Migration of the data in a smoothed background velocity produces the image shown in Figure 5(c). The zero-offset image trace is also superimposed on the image. As for the preceding example, we analyze the expression of model randomness on the image using log-log plots of the spectra, after we deconvolve the seismic wavelet from the image. Figure 7(a) displays the log-log spectrum of the zero-offset image trace. As before, we separate the k^{-1} component obtaining the spectrum shown in Figure 7(b). The linear least-squares fit to the image spectrum has a slope of 0.54, which is close to the slope obtained from the direct analysis of the well-log. Thus, we can conclude that the migrated image indicates the presence of a model with fractal parameter β approximately equal to 0.53. Figure 8 shows the dependence of extracted heterogeneity information from image on the horizontal position with respect to the source location. It is apparent that the extracted heterogeneity parameters in the near offset are more precise than in the far offset. We hypothesize that this fact most likely correlates with the angle of incidence at various reflectors, although the precise influence of the angle of incidence on the fractal parameters needs to be investigated further.

The procedure discussed here requires knowledge of the source wavelet to extract heterogeneity parameters from data or migrated images. However, only the amplitude spectrum matters, therefore we conjecture that we can still obtain satisfactory results even if small phase errors in our wavelet estimation exist.

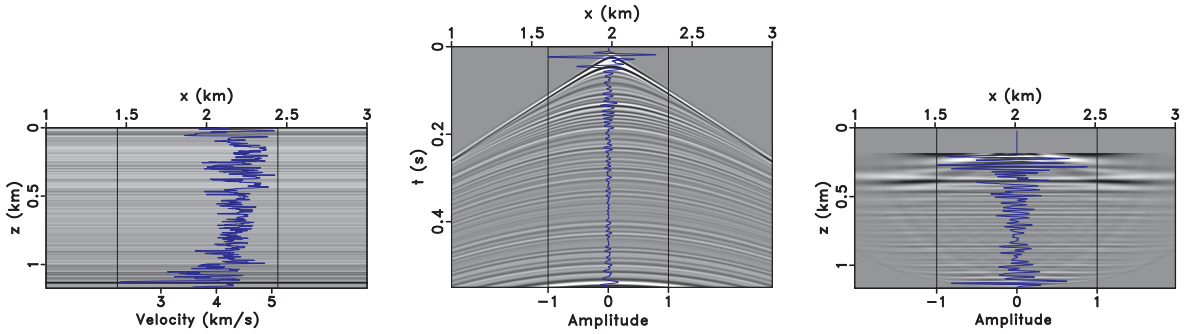

(a) (b) (c)

Figure 5: (a) Well-log of P-wave velocity extended horizontally to mimic a subsurface velocity model. (b) Data simulated in a shot-record experiment, with a shot at ($x = 2.0$ km, $z = 0$ km); the zero-offset trace is superimposed on the data. (c) Image of the data shown in Figure 5(b) using a conventional imaging condition and a smooth background velocity; the image trace at $x = 2.0$ km is superimposed on the image.

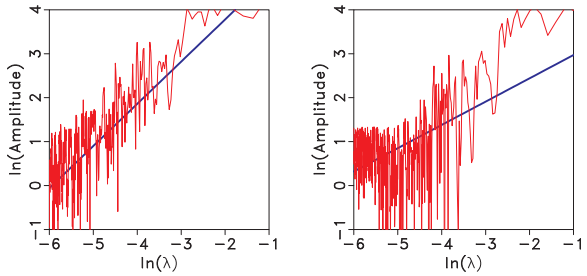

(a) (b)

Figure 6: (a) The log-log spectrum of the well log data. (b) The remaining spectrum after removing the k^{-1} component from the spectrum shown in (a). Thick lines show linear least-squares fits to the spectra.

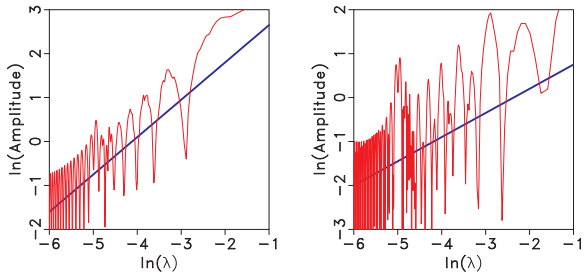

(a) (b)

Figure 7: The log-log spectrum analysis of (a) the zero-offset data trace and (b) the vertical image trace at $x = 2.0$ km after filtering to suppress the k^{-1} behavior. Thick lines show linear least-squares fits to the spectra.

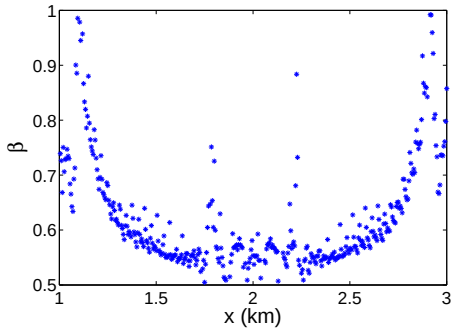

Figure 8: Extracted heterogeneity parameter β from the migrated image at various horizontal positions.

CONCLUSIONS

We compare different types of multi-scale heterogeneities and recover information about the parameters characterizing such models from the seismic data and migrated images. Our analysis shows that various types of heterogeneity have different character when analyzed in log-log plots. Assuming that the subsurface model is a combination of a relatively smooth background plus a few strong interfaces with a blocky character, we can attempt to infer the statistics of model heterogeneities currently undetectable by conventional seismic methodology. Heterogeneity information is available in data, as well as migrated images, but accessing this information requires reasonably good estimates of the source wavelet.

ACKNOWLEDGMENT

We acknowledge the support of the sponsors of the Center for Wave Phenomena at Colorado School of Mines. The well-log data was supplied by the Reservoir Characterization Project of the Colorado School of Mines.

REFERENCES

Claerbout, J. F., 1985, Imaging the Earth's interior: Blackwell Scientific Publications.

Dolan, S. S., C. J. Bean, and B. Riollet, 1998, The broad-band fractal nature of heterogeneity in the upper crust from petrophysical logs: Geophysical Journal International, **132**, 489–507.

Hoshiba, M., 2000, Large fluctuation of wave amplitude produced by small fluctuation of velocity structure: Physics of the earth and planetary interiors, **120**, 201–217.

Mandelbrot, B. B., 1982, The Fractal Geometry of Nature: Freeman, San Francisco.

Richter-Bernburg, G., 1987, Deformation within salt bodies in dynamincal geology of salt and related structures: Academic Press.

Shtatland, E. S., 1991, Fractal stochastic models for acoustic impedance: An explanation of scaling or 1/f geology and stochastic inversion: 61th Annual International Meeting, SEG, Expanded Abstracts, 1598–1601.

Stefani, J., and G. S. De, 2001, On the Power-Law Behavior of Subsurface Heterogeneity: 71th Annual International Meeting, SEG, Expanded Abstracts, 2033–2036.

Turcotte, D. L., 1997, Fractals and Chaos in Geology and Geophysics: Cambridge University Press.